Current **A**pplied **S**cience and **T**echnology e-ISSN: 2586-9396

Curr. Appl. Sci. Technol. 2025, Vol. 25 (No. 2), e0261045

Research article

Computational Investigation of Phytochemicals as Putative Inhibitors of *Vibrio parahaemolyticus* Protein Toxins

Jahangir Ahmed, Irfan Navabshan, and Karthikeyan Ramalingam*

School of Life Sciences, B.S. Abdur Rahman Crescent Institute of Science and Technology, Tamil Nadu, India

Received: 27 October 2023, Revised: 25 January 2024, Accepted: 7 October 2024, Published: 15 November 2024

Abstract

The lethal toxins released by pathogenic strains of *V. parahaemolyticus* pose a significant challenge in the aquaculture industry. One such toxin is thermostable direct haemolysin (TDH), which is encoded in the *tdh* gene. TDH primarily exerts its toxicity by creating pores in hemocyte membranes and other tissues. The *toxR* gene, on the other hand, plays a role in regulating the expression of virulence factors, including *tdh*, and is found in *Vibrio* species. Plants are recognized for containing phytochemicals that exhibit antibacterial properties with few adverse effects. This study acquired essential phytochemicals from PubChem, and target proteins from the RCSB protein data bank. The study was focused on the effects of alkaloids and flavonoid classes of phytochemicals on the target toxins measured by *in silico* (Gscore and MM/GBSA bind) investigation. This research employed *in silico* screening using Schrodinger's Glide, 2021 software, followed by a thorough analysis of how different phytochemicals interacted with specific binding sites, utilizing the Discovery Studio 3.5 version. Through this analysis, the most effective phytochemicals were identified, and myricetin (Myr) and (+)-taxifolin (TF) with ToxR, as well as chlorogenic acid (CGA) and carboxymethyl cellulose (CMC) with TDH, were analyzed. These phytochemicals displayed promising potential as inhibitors of the toxins, as evidenced by their docking scores and affinity. Among the compounds, Myr exhibited the best G-docking score at -6.004 Kcal/mol, followed by TF at -5.262 Kcal/mol against ToxR. Whereas, CGA and CMC also demonstrated notable scores at -5.245 Kcal/mol and -4.433 Kcal/mol against TDH, respectively. The *in silico* analysis suggested that these phytocompounds might have strong antibacterial properties against *V. parahaemolyticus* by effectively neutralizing these toxins. The screening results revealed several phytochemicals with promising docking scores and significant interactions with these toxins.

Keywords: in silico docking; *V. parahaemolyticus*; TDH; ToxR; toxins; molecular dynamic simulation

*Corresponding author: E-mail: karthikeyan.sls@crescent.education
https://doi.org/10.55003/cast.2023.261045

1. Introduction

Infections caused by the bacterium *Vibrio parahaemolyticus* can lead to various illnesses such as gastroenteritis, and, and in more severe cases, sepsis. The bacterium is a prevalent cause of bacterial gastroenteritis in Asia countries. The release of toxins, such as thermostable direct hemolysin (TDH) or TDH-related hemolysin (TRH), encoded by the *tdh* and *trh* genes, is a characteristic feature of pathogenic strains (El-Gamal & EL-Bahi, 2020). The *toxR* gene is a regulatory gene present in all *V. parahaemolyticus* strains, irrespective of the Kanagawa phenomenon, and can be identified using PCR techniques (Ali et al., 2023; Di Salvo et al., 2023). This gene encodes a membrane-bound regulatory protein that plays a significant role in consistent virulence emergence (Canals et al., 2023; Cohen et al., 2023) and was also found to be similar to *toxR* of *V. cholerae* (Simpson, 2023). The *toxR* gene also influences the expression of various other secretory system genes such as *tdh*, Type III secretion system 1 (T3SS1), and Type III secretion system 2 (T3SS2) genes (Canals et al., 2023; Hubbard et al., 2016). It was also found to repress T3SS1 gene transcription, possibly through direct activation of CalR, which is another T3SS1 repressor (Osei-Adjei et al., 2017). However, the direct regulatory effects of *toxR* on T3SS1 genes and the specifics of its actions on *tdh* and T3SS2 genes remain unknown. Researchers reported cell density-dependent *toxR* transcriptional patterns in *V. parahaemolyticus* and *V. cholerae* (Zhang et al., 2017), suggesting a potential relationship between *toxR* expression and quorum-sensing (QS) gene in pathogenic *Vibrios* spp. In *Vibrios* spp., *tdh* and *trh* genes were identified and found in 1-10% of environmental *V. parahaemolyticus* isolates (DePaola et al., 2000; Johnson et al., 2009). In another research in Japan and Chile, low densities of *tdh* and *trh* genes were reported (Alam et al., 2023). In India, the *tdh* gene was reported in 3% of environmental isolates, two isolates out of 71 in West Bengal, three isolates out of 61 in Andhra Pradesh, and one isolate out of 51 in Gujarat (Paria et al., 2019).

Other researchers studying *V. parahaemolyticus* virulence genes discovered three pathogenic islands (T3SS1, T3SS2, and T3SS6) responsible for producing various effector proteins with diverse functions. These proteins disrupt actin network, contribute to pathogen survival and reproduction within host cells, and aid in cell colonization (Matlawska-Wasowska et al., 2010). In the presence of a type VI secretory system, disease isolates suggest a potential fitness advantage for this opportunistic pathogen over other microorganisms in the same ecological niche. This phenomenon has the potential to significantly influence the process of colonization (Yang et al., 2019). T3SS, responsible for releasing cytotoxic and enterotoxic toxins, is crucial to the pathogenicity of *V. parahaemolyticus*. T3SS1, responsible for releasing cytotoxic proteins, was identified in nearly all isolates, while T3SS2 was typically found in clinical isolates encoding with *tdh* and/or *trh* genes (Kodama et al., 2008 Okada et al., 2009). It was recognized that the pathogenic islands of T3SS systems were critical in the pathogenicity of *V. parahaemolyticus* (Prithvisagar et al., 2021).

Phytocompounds, which have traditional medicinal values, play a significant role in therapeutic applications, exhibiting antibacterial, antiviral, and antifungal activities. They are also frequently employed for the enhancement of antibiotic activities. Myricetin, belonging to the flavonol class along with quercetin and kaempferol, is abundantly found in fruits, vegetables, tea, berries, and red wine, and contributes significantly to the nutraceutical value of these foods. Myricetin is well-recognized and has a characteristic pyrogallol B-ring. It also possesses a highly hydroxylated structure contributing to its superior biological properties compared to other flavonols, (Park et al., 2016). Myricetin

may be beneficial to the human central nervous system, and multiple research findings suggest its potential benefits in protecting against Parkinson's and Alzheimer's diseases. Modern pharmacological investigations have revealed its antibacterial, antiviral, antitumor, antioxidative, and anti-inflammatory properties. It also demonstrates the ability to protect lipids from oxidation, making it useful as a preservative to extend the freshness of food products that contain oils and fats (Semwal et al., 2016; Zhang et al., 2021). Taxifolin is an antibacterial substance isolated from numerous plants including *Acacia catechu*, conifers such as the Siberian larch, *Larix sibirica* in Russia, and Chinese yew. *Acacia catechu*, sometimes referred to as catechu, is a therapeutic shrub that serves several functions. The bark of this plant has strong anti-inflammatory, antibacterial, antifungal, and antioxidant properties (Hazra et al., 2010; Trishala et al., 2019). In addition to sore throats and diarrhoea, this plant extract has also been used to treat high blood pressure, colitis, digestive problems, bronchial asthma, cough, and leprosy (Lakshmi et al., 2021). The latest study examined its effects on the *V. parahaemolyticus* strain and discovered that TF exhibited antibacterial properties at a concentration of 1.25 mg/mL (Ahmed et al., 2023).

Another group of secondary metabolites, polyphenols, have received significant attention due to their useful biological effects (Díaz-Hernández et al., 2022). Among them, chlorogenic acid (CGA) has significant potential as a physiologically active substance, with its properties attributed to the presence of phenolic hydroxyl groups. Notably, CGA is characterized by its relatively low toxicity and minimal side effects. Due to its remarkable antibacterial, antioxidative, chemopreventive, and antioxidant properties, CGA, a phenolic compound naturally occurring in various herbs and in coffee and beans, is commonly referred to as the golden phytochemical (Lou et al., 2011; Huang et al., 2017). Carboxymethyl-cellulose (CMC), a frequently utilized cellulose derivative, is an anionic polysaccharide that readily dissolves in water. Its solution possesses the best film-forming properties and is devoid of toxicity. As a result, CMC finds application as an additive to improve the quality and processing attributes of materials employed in food packaging, such as food antifood spoilage agents (Ma et al., 2008; Dashipour et al., 2015).

The traditional screening of phytochemicals for use in therapeutic applications demands a lot of resources and time. With advancements in research, such as computer-aided drug design, offer a more efficient means for researchers to narrow down potential drug candidates, thereby saving time. This study provides insights into the molecular interactions and molecular dynamic simulation between phytochemicals and their target toxins (TDH and ToxR). Moreover, in this study, the selected phytochemicals exhibited promising results in docking when compared to antibiotics and demonstrate enhanced stability at molecular-level interactions between ligands and macromolecules. A synergistic effect of these compounds with conventional antibiotics may hold a potential approach to offer effective therapies against resistant strains of *V. parahaemolyticus* in the future.

2. Materials and Methods

2.1 Data collection

The phytocompounds were screened based on literature studies, and around 200 compounds were retrieved from the PubChem database (https://pubchem.ncbi.nlm.nih.gov) and saved as .sdf files. The ToxR protein homology modelling (trRosetta has been *used* to accurately design a novel *protein* structure) was performed to create crystal structure. Further, PROCHECK was used to analyze the stereochemical quality of

protein structures. The protein crystal structure for TDH (PDB: 3a57) was obtained from a protein data bank (PDB) (https://www.rcsb.org). The antibiotic gentamicin, used as a reference drug, was also retrieved and preserved for distinct docking studies, owing to its therapeutic promise and potential synergistic efficacy against bacterial infections (Liang et al., 2021). The docked phytocompounds .sdf was changed into pdb format using Open-Babel and saved in a common library.

2.2 Protein homology modelling

The ToxR protein was generated from the trRosetta (transform-restrained Rosetta) platform. Based on the alignment of the template protein sequences, homology modelling is used to predict the three-dimensional structure of a query protein. Furthermore, the structure conformation of ToxR allowed and disallowed regions of the designed protein were checked. In Figures1a and 1b, the PROCHECK server (structure validation server) was used to determine the Ramachandran plot for ToxR (Flores-Castañón et al., 2022). This method was used to analyze the stereochemical quality of the protein structure by evaluating plot statistics (Figure 1b). After analyzing, these criteria best-fit models were selected for further docking studies of the ToxR protein (Figure 1c). In Figure 1d, the protein crystal structure for TDH (PDB: 3a57) was retrieved from the protein data bank.

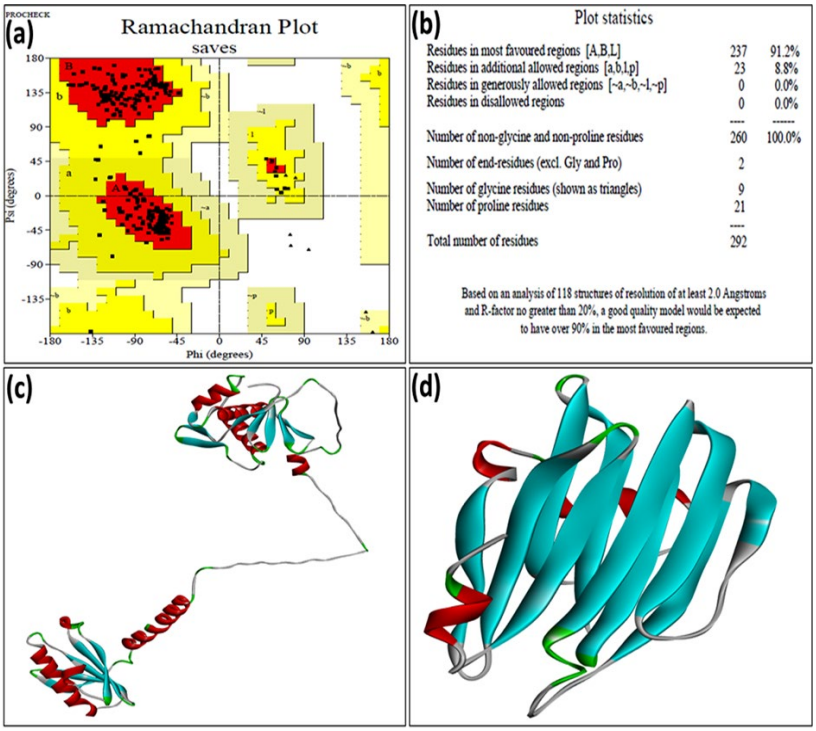

Figure 1. Demonstration of the crystal structures employed in the docking studies, comprising: ToxR homology modelling (ID-TR097850) structure and plots statistical analysis done by Procheck tool to confirm conformation through Ramachandran plot (a, b), selected ToxR model (c) and the selected crystal structure of TDH (PDB ID-3a57) obtained from protein data bank (d).

2.3 Ligand and protein preparation

A literature survey was used to identify the toxins of *V. parahaemolyticus* followed by homology modelling performed for ToxR, and the crystal structure of TDH was obtained from the protein data bank (PDB). The active sites for ToxR and TDH-toxin were identified with binding sphere radii of 7.5000 Å and 8.1622 Å, respectively, encompassing all active site amino acids surrounding the bound inhibitor, as shown in Table 1 and Figures 2a and 2b. After that, the protein was altered for Schrödinger-Maestro Prep wizard platform, which gave the calculations and preparation for glide docking (Glide 2021) (Rajagopal et al., 2020). Similarly, all water molecules were removed from the protein before docking. When all of the missing side chains were inserted, bond orders were assigned. Zero-order links to metals and the essential hydrogens for heavy atoms were introduced. Weaker limitations were executed on the non-hydrogen atoms. Continuous minimizations were performed using the OPLS4 force field until the non-hydrogen atoms' average root mean square deviation reached 0.3 Å (Hengphasatporn et al., 2020). This refinement process followed Schrödinger's recommended protocol (Rajagopal, et al., 2021). Compound structures retrieved were integrated into the Schrödinger Maestro workspace (Glide 2021). Subsequently, each structure had its bond order accurately assigned through the LigPrep program, and ionization states were determined using the Epik program at pH levels ranging from 2.0 to 7.0. Tautomers and protonation states may be automatically counted by LigPrep in the Schrödinger Suite by using Epik. The Inbuild Schrödinger Optimized Potentials for Liquid Simulations 4 (OPLS4) force field was utilized and optimized the inhibitors by examining five post-docking poses/ligands (Ferruzzi, 2010). The protonation and ionisation states of the ligand are often modified to meet the desired conditions of the docking experiment. This ensures that the ligand is in the correct conformation for binding to the target protein. So, proper ligand preparation is critical for generating reliable and effectual results in target molecule docking studies.

2.4 Virtual screening by docking

Schrodinger software (GLIDE module) was used to perform the computational docking. Before the molecular docking simulation, the protein binding site was examined. The receptor grid generation panel was set to the following XYZ coordinates: (18.7533, 2.7373, -0.8576) for ToxR, and (24.7135, 25.1987, 59.2414) for TDH. This setup generated a proper map, with the receptor grid-enclosing box centered to place active sites within the relevant protein 3D structure for docking. The conformational, structural, and functional characteristics of the docked ligand molecule were thoroughly searched by Glide. All (X, Y, and Z) coordinates were specified using the docking task option, and the ideal conformation of the ligand molecules was found using the scoring function (Gscore/MM/GBSA bind). For the final energy assessment, the glide score (Gscore/MM/GBSA bind) was used, and each ligand received a single ideal position as an output. Based on their ranked score (Gscore), the top phytocompounds docked against the ToxR, and TDH were selected for further study. The top candidates, with docking scores of -6.004 to -2.452 around this optimal threshold were expected to be more effective against each toxin. Additionally, higher negative values in terms of binding energy or binding affinity indicate better ligand performance. Greater energy release upon ligand binding to a protein suggests a stronger interaction. Here, a cumulative score for each protein-ligand complex was calculated taking into account factors such as robust and weak hydrogen bonds, hydrophobic interactions, salt bridges, and π-π interactions (Sajid et al.,

Table 1. The X, Y, and Z coordinate values of the protein binding site, as well as the diameter of the binding sphere. TDH-Thermostable Direct Haemolysin; PDB-protein data bank.

Protein PDB ID	Binding Sphere Radius (Å)	Coordinates (Å)		
		X	Y	Z
ToxR (ID TR097850)	7.5000	18.7533	2.7373	-0.8576
TDH (3A57)	8.1622	24.7135	25.1987	59.2414

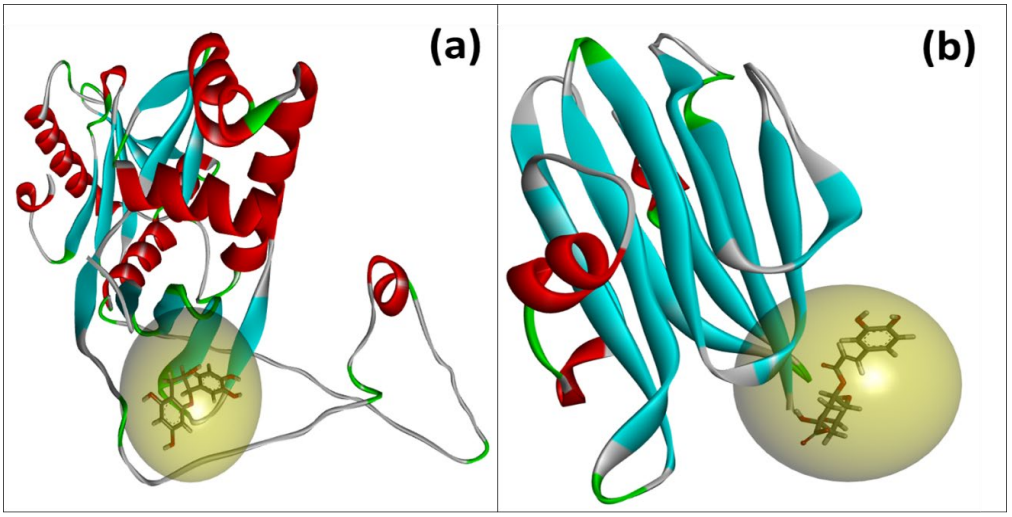

Figure 2. An illustration of the binding sphere radius for two protein toxins, namely, a) ToxR and b) TDH toxins, selected based on blind docking

Table 2. List of best phytochemicals Glide docking sores and MM/GBSA bind with ToxR protein and standard drug. CID- Compound ID number, MM/GBSA-Molecular mechanics generalized Born surface area.

S. No.	PubChem ID	Ligands	Glide Score (kcal/mol)	MMGBSA dG Bind Score
1	CID-5281672	Myricetin	-6.004	-25.08
2	CID-9064	Catechin	-5.956	-10.09
3	CID-5280343	Quercetin	-5.791	-23.53
4	CID-439533	Taxifolin	-5.262	-21.29
5	CID-5280805	Epigallocatechin gallate	-5.212	-13.19
Glide docking score with standard drug				
6		Gentamicin	-6.088	-41.08

2022). This process resulted in a ranking that reflected the expected stability of the assessed complexes. Such analyses enhanced the affinity of the docking results, reducing reliance on individual affinity scores, as depicted in Tables 2 and 3. The selection of compounds for *in-silico* output was determined by their antibacterial activity from previous studies (Hazra et al., 2010; Park et al., 2016; Semwal et al., 2016; Trishala et al., 2019; Lakshmi et al., 2021; Zhang et al., 2021; Díaz-Hernández et al., 2022; Ahmed et al., 2023).

Table 3. List of best phytochemicals Glide docking scores and MM/GBSA bind score with TDH toxin (PDB: 3a57), and a standard drug. CID-Compound ID number, MM/GBSA-Molecular mechanics generalized Born surface area.

S. No.	PubChem ID	Ligands	Glide Score (kcal/mol)	MMGBSA dG Bind Score
1	CID-1794427	Chlorogenic acid	-5.245	-18.47
2	CID-23706213	Carboxymethyl cellulose	-4.433	-21.52
3	CID-72	3,4-Dihydroxybenzoic acid	-3.533	-6.17
4	CID-23111554	Poly (Lactide-Co-Glycolide)	-2.694	-8.26
5	CID-4788	Phloretin	-2.452	-22.58

2.5 Docking protocol validation

In this study, we conducted separate observations of the 2D and 3D structures of the protein-ligand complex using validation methods. This involved the use of various parameter sets to impose specific constraints. These constraints included metal constraints to account for coordination geometries, hydrogen bond constraints for interactions with particular functional groups on the receptor, positional constraints to place docked poses within a defined spatial relationship to the receptor, and hydrogen bond constraints for interactions with specific functional groups (Rajagopal, et al., 2020). This method also involved drawing out the structures of reference inhibitor (gentamicin) and using Schrödinger-Maestro software to individually minimize each molecule's potential energy. Furthermore, we conducted separate docking studies of these compounds against the ToxR/TDH targets to calculate their binding energies (Gdocking score). We evaluated top-priority docked compounds based on well-established benchmarks and compared the activity values of these molecules with the corresponding results extracted from Glide docking energy files (both selective and nonselective) (Ahmed et al., 2023).

3. Results and Discussion

3.1 Docking analysis

The results of the Gdocker protocol tracks were analyzed. These observations were crucial to determining the active site binding pocket variations within protein toxins (ToxR and TDH). Utilizing Schrodinger for docking, the top phytochemical compounds, along with a standard drug, were identified as efficient interactors with ToxR and TDH protein toxins. Subsequently, we assessed the molecular interaction results obtained from the docking

experiments, considering crucial parameters including final intermolecular energy, inhibition constants, and the formation of hydrogen bonds during the docking process between ligands and receptor molecules (Yadav et al., 2023).

3.2 Minimization models analysis

In computational structural biology and molecular modelling, protein superimposition is a typical process that occurs before and after energy minimization. Utilizing molecular mechanics force fields, energy minimization is used to optimize the atomic locations in protein structures (Jacobson et al., 2004). Here, we utilized the Schrodinger inbuilt OPLS (Optimized Potentials for Liquid Simulations) force field for protein energy minimization-based structure development. This can relax the structure and get rid of steric conflicts and other structural flaws. Here is an example of how superimposition and energy conservation might be combined (Rohl et al., 2004). After minimization, the superimposed model residual differences were noted with ToxR-ToxR proteins as Thr24, Thr27, and Thr25; and Val114, Gly115, Glu116, Lys155, Glu156, and Ser157 in the loop-to-helix changes in Figures 3a-c. Additionally, the TDH-TDH proteins superimposed loop-to-helix residual differences were noted as Gly67, Arg65, and Gly68, and also at Ala136, Ser137, Asp138, Ile142, Thr143, and Ile144, in Figures 3d-3e.

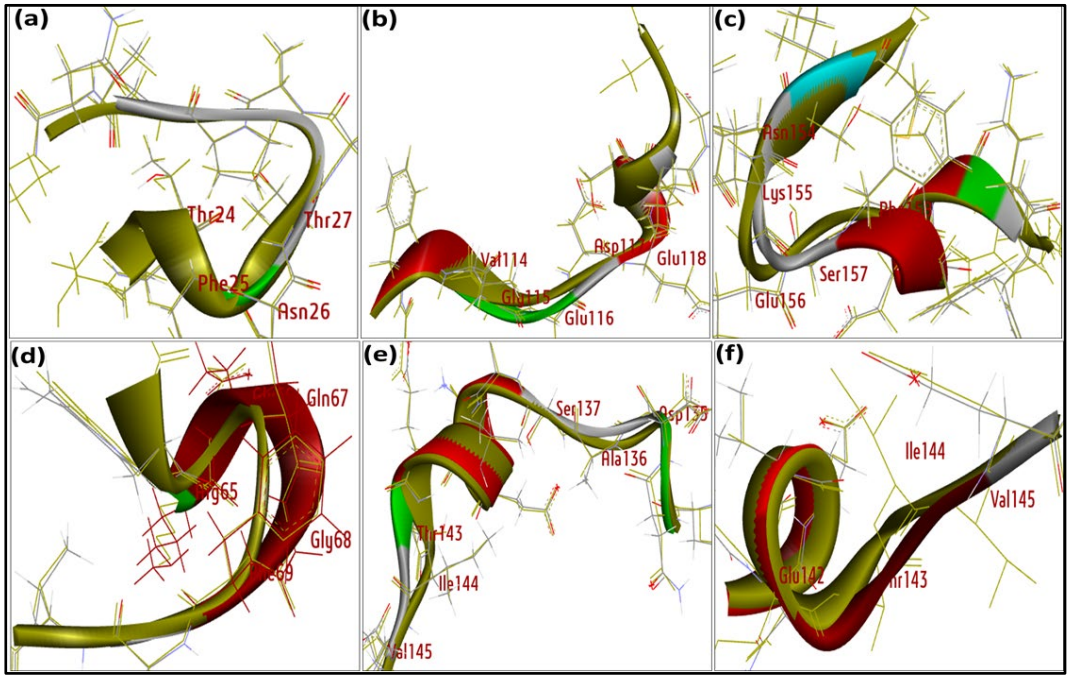

Figure 3. Maxima and minima model analysis of ToxR (a, b, c) and TDH (d, e, f) protein toxins of *V. parahaemolyticus*. The identical protein superimposes model energy minimization processes, there were conformational changes in the protein transitioning from a helical to a loop structure with residual difference.

3.3 Docking studies of the reference drug with ToxR/Tdh toxin

Gentamicin interacts with the ToxR receptor, a complex assembly characterized by polar amino acids (a/a) (Liang et al., 2021). This interaction is particularly captivating due to the presence of two crucial hydrogen bonds established at ASN19 and ASN21, both of which serve as donor interactions. Additionally, two salt bridge interactions have been identified, featuring negatively charged amino acids at GLY125 and ASP17, as visually depicted in Figure 4. This interaction yields a substantial docking score of -6.088 kcal/mol, a reflection of the binding affinity between the two entities. A comprehensive overview of the outcomes derived from the gentamicin-ToxR docking analysis is presented in Table 2 and Figure 4.

Importantly, it has been established that not all amino acid residues within the ToxR toxin actively participate in hydrogen bonding and other kinds of interactions. Instead, only two hydrogen bonds and two salt bridge interactions have been identified within the active site of the ToxR protein. Current research on drug usage has shown that selected antibiotics do not show any docking interactions with the TDH toxin (G-dock and MM/GBSA). To create more successful treatment options for bacterial infections caused by toxin-producing bacteria, it is critical to research and understand the unique interactions between antibiotics and toxins like TDH toxin. This research can assist in determining which phytochemical derivatives are most effective against certain bacteria, which could lead to the development of new medicines or antibiotic combinations to challenge such infections (Panwar et al., 2023).

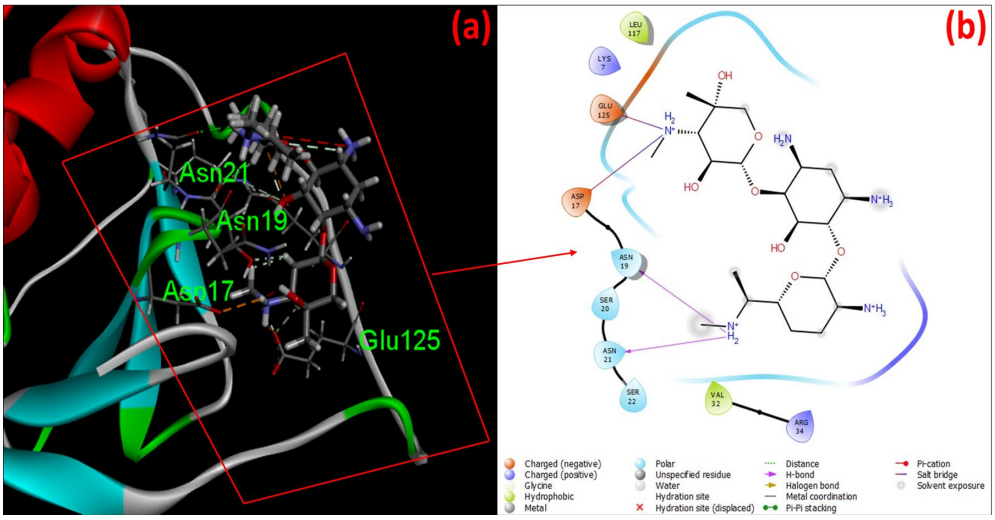

Figure 4. Binding-interaction of 3D model of standard drug (gentamicin) with (a) ToxR, and (b) 2D model analysis

3.4 Docking analysis with toxR

Among the docked compounds, myricetin and taxifolin exhibited a better binding affinity with the ToxR protein toxin than the other phytochemicals. Myricetin and taxifolin were accurately positioned within the catalytic site of the ToxR-RBD (Receptor Binding Domain). This binding was facilitated by negatively charged interacting residues at ASP17 and GLU127, along with hydroxyl group interactions. Notably, the hydroxyl group at the terminal

end of the ToxR receptor engaged in a hydrogen bond interaction with SER118, forming a bi-furcated donor interaction. Additionally, SER123 participated in a hydrogen bond interaction with another ring. These findings highlight the successful binding interactions (Figure 4ab) (Ferreira et al., 2015). Therefore, myricetin was mostly linked to the binding position through hydrogen bonds and a docking score of -6.004 Kcal/mol, and important H-bonds interactions are tabulated in Tables 2 and 4. Figure 5a depicts the 3D model analysis, whereas Figure 5b shows the 2D interactional analysis of the myricetin-ToxR toxin complex. The hydroxyl group in the terminal ToxR ring with taxifolin exhibited bi-furcated acceptor and donor H-bonding with LYS7; ASP17 and the hydroxyl group of another terminal showed bi-furcated donor H-bonds interaction with SER127. Two forms of negatively charged amino acids, ASP and GLU, were observed interacting through hydrogen bonding within the binding pocket (XYZ-18.7533, 2.7373, -0.8576), along with two forms of polar amino acids, ASN and SER, resulting in a ToxR-taxifolin docking score of -5.262 kcal/mol. Taxifolin demonstrated all the hydrogen-bond interactions, which were identified with the backbone of the ToxR protein toxin as depicted in Figure 5 (Raj & Varadwaj, 2016). Figure 5c illustrates the 3D interaction analysis, while Figure 5d presents the 2D interaction analysis of taxifolin with the ToxR protein.

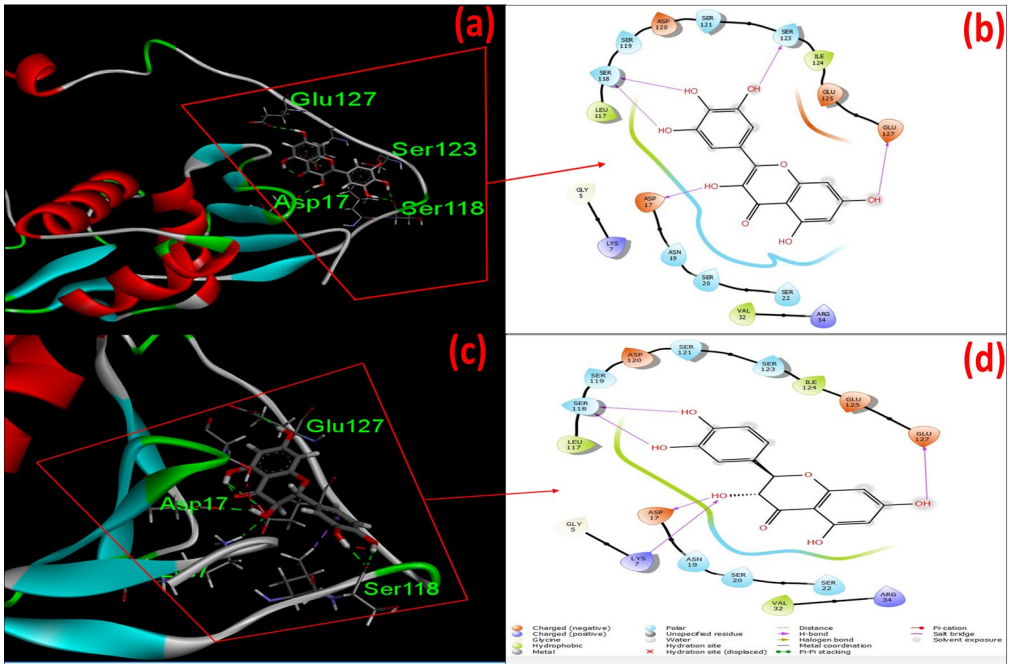

Figure 5. 3D and 2D binding-interaction of ToxR-Myricetin complex (a, b) and ToxR-Taxifolin complex (c, d) analysis.

Table 4. Types of hydrogen bonds interaction involved with the active site of ToxR protein

S. No	Ligand	H-Bond Interaction	H-BA	H-BD	Total H-bonds
1	Myricetin	Asp19, Ser118, Ser123, Glu127	-	5	5
2	Quercetin	Ser20, Glu127, Glu125, Ser118	1	4	5
3	Catechin	Lys7, Asp17, Ser22, Ser118, Glu127	1	5	6
4	Taxifolin	Lys7, Asp17, Ser118, Glu127	1	4	5
5	Epigallocatechin gallate	Asn19, Ser118, glu125, Glu127	1	4	5
	Binding interaction of standard Antibiotics with the active site of ToxR Toxin				
6	Gentamicin	Asn19, Asn21	-	2	2

3.5 Docking analysis with TDH (PDB ID: 3a57)

All the terminal phenyl and oxyphenyl rings of chlorogenic acid were found to be correctly buried into the exterior concave surface of RBM (Receptor binding motif) and stabilized by three hydrogen bonds, one salt bridge, and one pi-cation interaction. Chlorogenic acid was correctly positioned into the catalytic site assembled by positively charged residues as SER13, SER61, and SER144, and the salt bridge interacts at GLY12 and pi-cation at LYS45 with Gdocking score of -5.245 Kcal/mol. The hydroxyl group of the terminal TDH ring with chlorogenic acid hydrogen bond interacts at SER61 and SER144, as shown in Figures 6a and 6b. Whereas the oxyphenyl ring of ToxR interacted with GLY12 and SER13. On the other hand, LYS45 interacted centrally with the TDH ring. The results of the docking score and total important H-bond interactions are tabulated in Tables 3 and 5. Carboxymethyl cellulose was properly surrounded by polar residues SER142 and SER144 and no other interactions were observed, with docking energy -4.433 kcal/mol. The hydroxyl group on the terminal phenyl ring exhibited a trifurcated hydrogen-bonding interaction with SER142, involving all types of donor interactions. Furthermore, the hydroxyl group on the terminal oxyphenyl ring established an acceptor interaction with SER144. These interactions played a key role at the binding site of TDH-CMC, as shown in Figures 6c and 6d). Our best-docked phytocompounds showed successful interaction against ToxR/TDH toxins, which may be helpful for the reduction of *V. parahaemolyticus* toxin load in shrimp aquaculture (Piplani et al., 2018; Soto-Rodriguez et al., 2022). This is likely because phytocompounds have shown medicinal properties historically, and research has found that antibiotic resistance can be reversed using these phytochemicals from various chemical groups. In addition to having direct antibacterial properties, some of these compounds have been shown to have synergistic effects (*in-vitro*) when used in combination with conventional antibiotics. In light of these findings, phytochemicals can be shown therapeutically as a valuable source of phytocompounds with antibacterial properties (Cao et al., 2020).

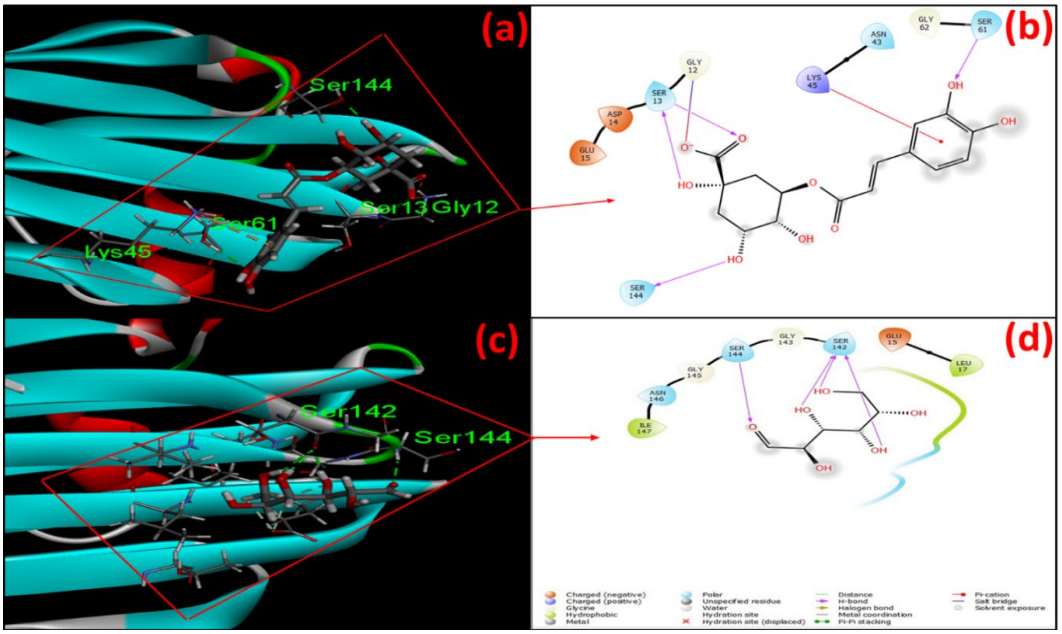

Figure 6. 3D and 2D binding interaction of TDH-chlorogenic acid complex analysis (a, b), and TDH-carboxymethylcellulose complex (c, d)

Table 5. Types of hydrogen bond interaction involved with the active site of TDH toxin (PDB ID: 3a57)

S. No.	Ligand	H-Bond Interaction	H-BA	H-BD	Total H-Bonds
1	Chlorogenic acid	Gly12, Ser13, Ser61, Ser144	2	2	4
2	Carboxymethyl cellulose	Ser144, Ser142	1	3	4
3	3,4 Dihydroxybenzoic acid	Gly12, Lys64, Ser144	1	1	2
4	PLGA (Poly (lactic-co-glycolic acid)	Asn41, Agr42, Asn43, Thr62	3	1	4
5	Phloretin	Glu15, Ser13, Ser144	1	3	4

3.6 RMSD and RMSF plot of protein-ligand complexes

Analysing protein compactness and root-mean-square deviation (RMSD) measurements with respect to time are essential because they show the general stability of docked complexes when ligands are bound (Azam et al., 2012). The lowest level of variation in RMSD values indicates greater protein and protein-ligand complex stability. In Figure 7a, the root-mean-square deviation graph of the ToxR-myricetin complex is shown over a timeframe of 100 nanoseconds (ns). In Figure 7a, at the initial time scale from 0 to below 20 ns, the RMSD of ToxR vastly fluctuated closely in a range of 15 to 24 Å. After 21 ns, it

decreased and fluctuated in the range of 24 to 25 Å up to 70 ns. Moreover, an increase in the RMSD values was seen from 24 to 27 Å in the time range of 90 to 100 ns, and a reduction was observed up to the end of 20 ns. In Figure 7b, the RMSF value of the ToxR-myristicin complex was primarily noted to be in fluctuation mode between the values of 10 to 20 Å up to 250 residues. Thereafter, it increased, and a decrease was observed in the fluctuation all along reaching up to 100 ns. In Figure 7c, the RMSD graph of TDH-chlorogenic acid complex is shown with a timeframe of 100 ns. In Figure 7c, at the initial time scale from 0 to 20 ns, the RMSD of TDH was found to fluctuate in the range of 0.9 to 1.2 Å. After 20 to 35 ns, it showed more increase in fluctuation between the range from 1.5 to 2.4 Å up to 40 ns. Additionally, no more increase and decrease in the RMSD values were seen between 1.8 to 2.1 Å over the time range of 45 to 100 ns, and this complex was observed more stable compared to ToxR as well as the reference drug.

The root-mean-square fluctuation (RMSF) was adopted for exploring the numerical measurement and computation analysis of individual residual flexibilities that were noticed in this study; minimal coordinate fluctuation indicates the highest stability. In Figure 7d, the RMSF of the TDH-chlorogenic complex is shown with the fluctuating peaks analyzed. Significantly less fluctuation was observed at amino acids 30-40, 45, 65, and 130 to 135 residues followed by more than 80 residues within a range of 0.1 to 0.8 Å and 0.1 to 1.8 Å. Likewise, the RMSD of reference drug results are shown in Figures 7e and 7f, respectively. In Figure 7e, for the toxR-gentamicin complex, the RMSD was observed to fluctuate in the ranges of 0 to 18 Å with a time scale of 0 to 25 ns. At a later stage, it showed a decrease from 20 to 23 Å at 25 ns and showed a rise with a steep increased fluctuation from 17 to 30 Å up to the end time points. On the other hand, the RMSF of the ToxR-gentamicin (reference drug) complex, shown in Figure 7f, exhibited higher fluctuations between residues 0 to 2, 20 to 40, and from 120 to 150, reaching up to 16 Å fluctuations during the whole simulation period of 100 ns. Our results, with particular emphasis, showed that the RMSF and RMSD of the TDH-chlorogenic acid complex were stable over the whole sequence compared to the reference drug. The acquired data points and/or values in this context have demonstrably shown that the RMSD of ToxR-myristicin complex was found to be less fluctuation in simulation over 100 ns compared to the reference drug. Additionally, more stability was observed with the TDH-chlorogenic acid complex compared to the reference drug. Therefore, we hypothesize that the screened compounds might at clinical stage inhibit or control the *toxR/Tdh* pathways of *V. parahaemolyticus*.

3.7 Contact histogram analysis of protein-ligand complexes

Protein-ligand contacts, including hydrogen bonds, hydrophobic, water bridges, and van der Waals forces interactions are important. Consideration of hydrogen-bonding properties in drug design due to their strong influence on drug specificity, metabolism, and absorption. An analysis of these interactions helps in understanding the key residues involved in binding, the strength of these interactions, and the overall stability of the complex. It is an important tool in structural protein engineering and drug design because it identifies important points of interaction that can be targeted to improve binding affinity or specificity. A heat map contact histogram of ToxR-myristicin is shown in Figure 8a and 8b, and a high number of hydrogen contacts was observed. In Figure 8a, protein–ligand contact frequently involved residues Ilu4, lys7, Asp17, Ser122, Gly125, and Glu127 over a substantially shorter time frame and contacts were discovered to be constant in loss and gain contacts of 20-40 ns and 60-70 ns. Finally, for the ToxR-myristicin complex, strong hydrogen bonding interactions were noted for lys7, Asp17, Ser122, and Glu125, as shown in Figure

8b. Typically, with hydrogen bonds and water bridges, amino acid residues were noted as Gly12, Asp14, Glu15, Lys64, Glu141and Gly143, among which Gly12 and Glu15 formed strong hydrogen bonds in comparison to other residues. The heat map of the TDH-chlorogenic acid complex revealed a greater number of contacts, indicated by darker bands, for Gly12 and Glu15. Interestingly, there were no observed changes in contact status between 0 and 100 ns, as seen in Figure 8c. Figure 8d illustrates the protein-ligand contacts in the TDH-chlorogenic acid complex, with consistent loss and gain of contacts observed for Gly12 and Glu15 over a relatively short time period ranging from 0 to 100 ns. Finally, in the case of gentamicin (reference drug), the heat map histogram in Figure 8e shows that Glu125 and Glu127 had strong hydrogen bond interactions during the simulation for time sale at up to 100 ns. The loss of contact at 0-5 ns and gain in contact at 10-100 ns were observed. The strong hydrogen bonding with Glu125 and Glu127 was observed in Figure 8f.

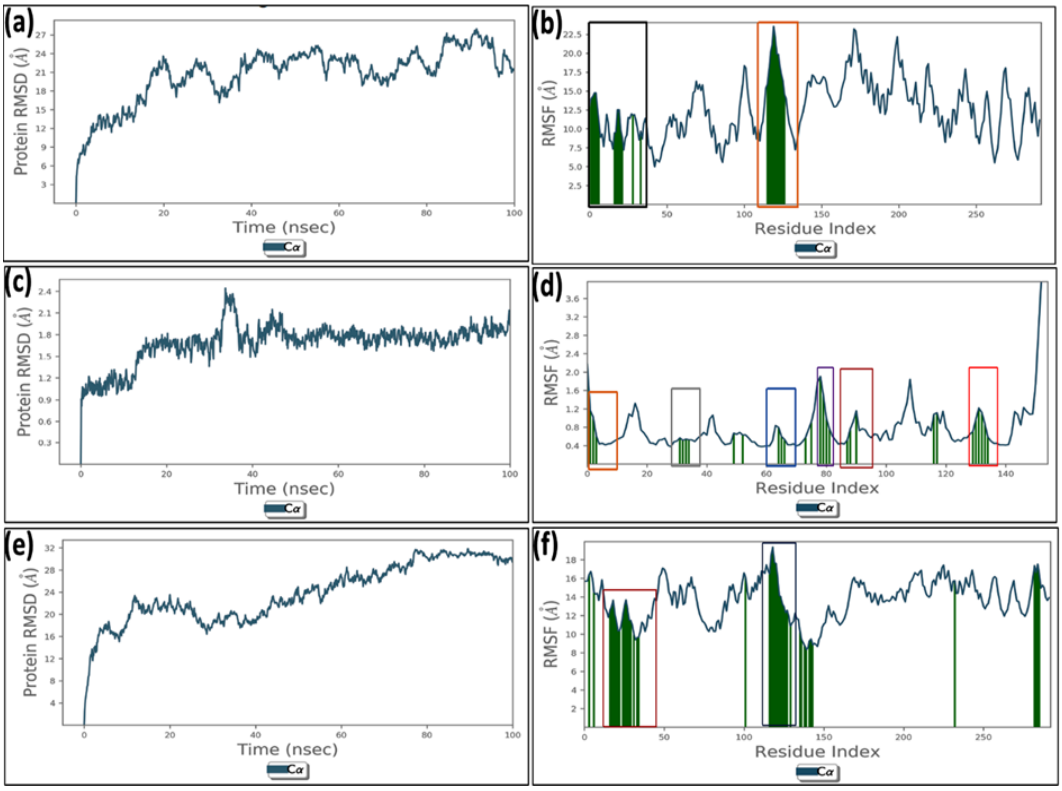

Figure 7. RMSD of ToxR-myricetin complex and RMSF (a, b), RMSD of TDH-chlorogenic acid and RMSF (c, d), RMSD of toxR-gentamicin complex (e, f) at 100 ns

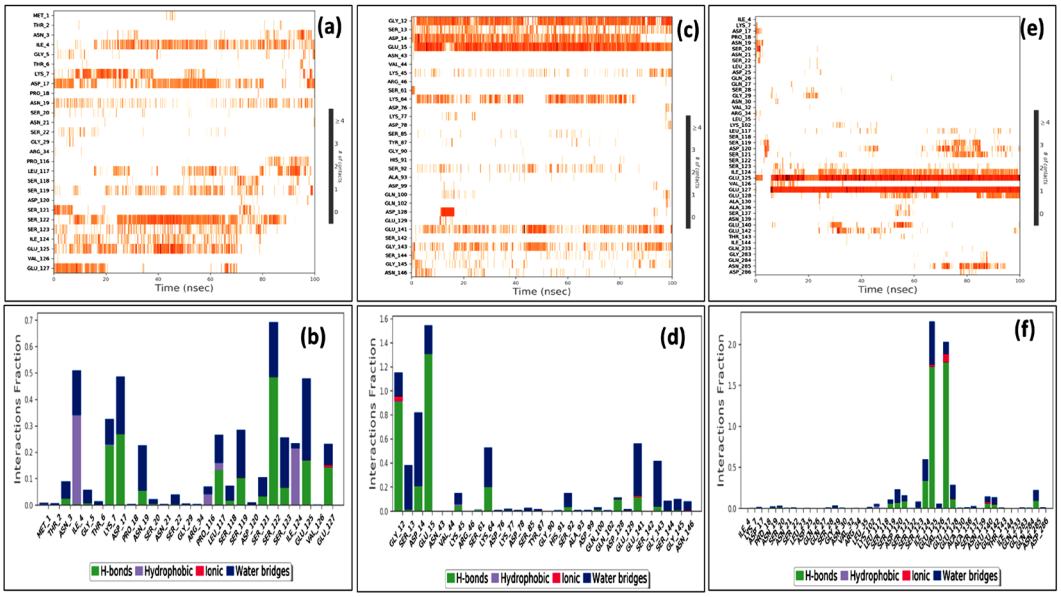

Figure 8. The contact histogram of Protein–ligand of ToxR-myristicin (a, b); TDH-chlorogenic acid (c, d) and antibiotics (reference drug) ToxR-gentamicin complexes (e, f)

4. Conclusions

Pathogenic bacteria secrete bacterial toxins (both exotoxins and endotoxins) into the gastrointestinal tracts of shrimp and fish, leading to lethal diseases. In light of the challenges posed by antibiotic resistance, researchers have been working on developing effective and sustainable solutions to address these issues. This study was focused on the assessment of the potential of naturally derived phytocompounds myricetin, taxifolin, chlorogenic acid, and carboxymethylcellulose as antibacterial agents. The investigation revealed that these phytocompounds exhibited individual interactions with the toxins and achieved favourable docking scores *in-silico*, indicating their capacity to effectively inhibit the toxins produced by *V. parahaemolyticus*. Gdocking score for myricetin of -6.004 Kcal/mol, closely followed by (+)-taxifolin (TF) at -5.262 Kcal/mol in their interaction with ToxR were observed. In the case of TDH, chlorogenic acid (CGA) and carboxymethyl cellulose (CMC) also displayed notable Gdocking scores of -5.245 Kcal/mol and -4.433 Kcal/mol, respectively. The "*in silico*" screening results revealed a selection of phytochemicals with promising Gdocking scores and substantial interactions with these protein toxins, opening up paths for further research for potential therapeutic applications. Utilizing a combination of theoretical bioinformatics and experimental validation offers a significant reduction in both the time and costs associated with the screening process. Likewise, adopting a combinatorial approach for aquaculture development represents an essential progression for this industry, which is valued in the millions. This approach holds a significant interest in research to find novel phytochemicals as a potential treatment and may open new ways for a broader range of bacterial therapies in the future.

5. Acknowledgements

We acknowledge B.S. Abdur Rahman Crescent Institute of Science and Technology for providing the facility to perform this research. This work was supported by the Indian Council of Medical Research [Project ID: 2020-4964]. The authors would like to thank the Research Funding Board, Indian Council of Medical Research.

6. Conflicts of Interest

The authors declare no conflicts of interest.

ORCID

Jahangir Ahmed https://orcid.org/0000-0002-1380-939X

Irfan Navabshan https://orcid.org/0000-0003-4630-5259

Karthikeyan Ramalingam https://orcid.org/0000-0002-9334-427X

References

Ahmed, J., Navabshan, I., Unnikrishnan, S., Radhakrishnan, L., Vasagam, K. P. K., & Ramalingam, K. (2023). In silico and in vitro investigation of phytochemicals against shrimp AHPND syndrome causing PirA/B toxins of *Vibrio parahaemolyticus*. *Applied Biochemistry and Biotechnology*, 195(12), 7176-7196. https://doi.org/10.1007/s12010-023-04458-1

Alam, M. J., Miyoshi, S. I., & Shinoda, S. (2003). Studies on pathogenic *Vibrio parahaemolyticus* during a warm weather season in the Seto Inland Sea, Japan. *Environmental Microbiology*, 5(8), 706-710. https://doi.org/10.1046/j.1462-2920.2003.00458.x

Ali, E. A., Al-azeem, M. W. A., & Younis, W. (2023). Microbiological and molecular characterization of *Vibrio cholera* and *Vibrio parahaemolyticus* isolated from Tilapia fish (*Oreochromis niloticus*). *SVU-International Journal of Veterinary Sciences*, 6(3), 1-16. https://doi.org/10.21608/svu.2023.203762.1266

Azam, S. S., Uddin, R., & Wadood, A. (2012). Structure and dynamics of alpha-glucosidase through molecular dynamics simulation studies. *Journal of Molecular Liquids*, 174, 58-62. https://doi.org/10.1016/j.molliq.2012.07.003

Canals, A., Pieretti, S., Muriel-Masanes, M., Yaman, N. E., Plecha, S. C., Thomson, J. J., Fàbrega-Ferrer, M., Pérez-Luque, R., Krukonis, E. S., & Coll, M. (2023). *ToxR* activates the *Vibrio cholerae* virulence genes by tethering DNA to the membrane through versatile binding to multiple sites. *Proceedings of the National Academy of Sciences,* 120(29), Article e2304378120. https://doi.org/10.1073/pnas.2304378120

Cao, H., Li, X., Wang, F., Zhang, Y., Xiong, Y., & Yang, Q. (2020). Phytochemical-mediated glioma targeted treatment: drug resistance and novel delivery systems. *Current Medicinal Chemistry*, 27(4), 599-629. https://doi.org/10.2174/0929867326666190809221332

Cohen, H., Fridman, C. M., Gerlic, M., & Salomon, D. (2023). A *Vibrio* T6SS-mediated lethality in an aquatic animal model. *Microbiology Spectrum*, 11(4), Article 0109323. https://doi.org/10.1128/spectrum.01093-23

Dashipour, A., Razavilar, V., Hosseini, H., Shojaee-Aliabadi, S., German, J. B., Ghanati, K., Khakpour, M., & Khaksar, R. (2015). Antioxidant and antimicrobial carboxymethyl cellulose films containing *Zataria multiflora* essential oil. *International Journal of Biological Macromolecules*, 72, 606-613. https://doi.org/10.1016/j.ijbiomac.2014.09.006

DePaola, A., Kaysner, C. A., Bowers, J., & Cook, D. W. (2000). Environmental investigations of Vibrio parahaemolyticus in oysters after outbreaks in Washington, Texas, and New York (1997 and 1998). *Applied and Environmental Microbiology*, 66(11), 4649-4654. https://doi.org/10.1128/AEM.66.11.4649-4654.2000

Di Salvo, E., Panebianco, F., Panebianco, A., & Ziino, G. (2023). Quantitative detection of viable but nonculturable *Vibrio parahaemolyticus* in frozen bivalve molluscs. *Foods*, 12(12), Article 2373. https://doi.org/10.3390/foods12122373

Díaz-Hernández, G. C., Alvarez-Fitz, P., Maldonado-Astudillo, Y. I., Jiménez-Hernández, J., Parra-Rojas, I., Flores-Alfaro, E., Salazar, R., & Ramírez, M. (2022). Antibacterial, antiradical and antiproliferative potential of green, roasted, and spent coffee extracts. *Applied Sciences*, 12(4), Article 1938. https://doi.org/10.3390/app12041938

El-Gamal, A. M., & EL-Bahi, E. F. (2020). Prevalence of *Vibrio parahaemolyticus* in seabass (*Dicentrarchus labrax*) and seabream (*Sparus aurata*) and detection of streptomycin-resistant strains. *World Veterinary Journal*, 10(3), 325-331.

Ferreira, L. G., Dos Santos, R. N., Oliva, G., & Andricopulo, A. D. (2015). Molecular docking and structure-based drug design strategies. *Molecules*, 20(7), 13384-13421. https://doi.org/10.3390/molecules200713384

Ferruzzi, M. G. (2010). The influence of beverage composition on delivery of phenolic compounds from coffee and tea. *Physiology and Behavior*, 100(1), 33-41. https://doi.org/10.1016/j.physbeh.2010.01.035

Flores-Castañón, N., Sarkar, S., & Banerjee, A. (2022). Structural, functional, and molecular docking analyses of microbial cutinase enzymes against polyurethane monomers. *Journal of Hazardous Materials Letters,* 3, Article 100063. https://doi.org/10.1016/j.hazl.2022.100063

Hazra, B., Sarkar, R., Biswas, S., & Mandal, N. (2010). The antioxidant, iron chelating and DNA protective properties of 70% methanolic extract of' Katha'(Heartwood extract of Acacia catechu). *Journal of Complementary and Integrative Medicine*, 7(1). https://doi.org/10.2202/1553-3840.1335

Hengphasatporn, K., Garon, A., Wolschann, P., Langer, T., Yasuteru, S., Huynh, T. N., Chavasiri, W., Saelee, T., Boonyasuppayakorn, S., & Rungrotmongkol, T. (2020). Multiple virtual screening strategies for the discovery of novel compounds active against dengue virus: A hit identification study. *Scientia Pharmaceutica*, 88(1), Article 2. https://doi.org/10.3390/scipharm88010002

Huang, Y., Chen, H., Zhou, X., Wu, X., Hu, E., & Jiang, Z. (2017). Inhibition effects of chlorogenic acid on benign prostatic hyperplasia in mice. *European Journal of Pharmacology*, 809, 191-195. https://doi.org/10.1016/j.ejphar.2017.04.017

Hubbard, T. P., Chao, M. C., Abel, S., Blondel, C. J., Abel zur Wiesch, P., Zhou, X., Davis, B.M., & Waldor, M. K. (2016). Genetic analysis of *Vibrio parahaemolyticus* intestinal colonization. *Proceedings of the National Academy of Sciences*, 113(22), 6283-6288. https://doi.org/10.1073/pnas.1601718113

Jacobson, M. P., Pincus, D. L., Rapp, C. S., Day, T. J., Honig, B., Shaw, D. E., & Friesner, R. A. (2004). A hierarchical approach to all-atom protein loop prediction. *Proteins: Structure, Function, and Bioinformatics*, 55(2), 351-367. https://doi.org/10.1002/prot.10613

Johnson, C. N., Flowers, A. R., Young, V. C., Gonzalez-Escalona, N., DePaola, A., Noriea, N. F., & Grimes, D. J. (2009). Genetic relatedness among *tdh+* and *trh+ Vibrio parahaemolyticus* cultured from Gulf of Mexico oysters (Crassostrea virginica) and surrounding water and sediment. *Microbial Ecology,* 57, 437-443. https://doi.org/10.1007/s00248-008-9418-3

Kodama, T., Hiyoshi, H., Gotoh, K., Akeda, Y., Matsuda, S., Park, K. S., Cantarelli, V. V., Iida, T., & Honda, T. (2008). Identification of two translocon proteins of *Vibrio parahaemolyticus* type III secretion system 2. *Infection and Immunity*, 76(9), 4282-4289. https://doi.org/10.1128/iai.01738-07

Lakshmi, T., Roy, A., & George, R. S. (2021). Antibacterial activity of *Acacia catechu* seed against urinary tract pathogens. *Journal of Complementary Medicine Research*, 11(5), 123-123.

Liang, F., Sun, C., Li, S., Hou, T., & Li, C. (2021). Therapeutic effect and immune mechanism of chitosan-gentamicin conjugate on Pacific white shrimp (*Litopenaeus vannamei*) infected with *Vibrio parahaemolyticus*. *Carbohydrate Polymers*, 269, Article 118334. https://doi.org/10.1016/j.carbpol.2021.118334

Lou, Z., Wang, H., Zhu, S., Ma, C., & Wang, Z. (2011). Antibacterial activity and mechanism of action of chlorogenic acid. *Journal of Food Science*, 76(6), M398-M403. https://doi.org/10.1111/j.1750-3841.2011.02213.x

Ma, X., Chang, P. R., & Yu, J. (2008). Properties of biodegradable thermoplastic pea starch/carboxymethyl cellulose and pea starch/microcrystalline cellulose composites. *Carbohydrate Polymers*, 72(3), 369-375. https://doi.org/10.1016/j.carbpol.2007.09.002

Matlawska-Wasowska, K., Finn, R., Mustel, A., O'Byrne, C. P., Baird, A. W., Coffey, E. T., & Boyd, A. (2010). The *Vibrio parahaemolyticus* Type III Secretion Systems manipulate host cell MAPK for critical steps in pathogenesis. *BMC Microbiology*, 10, Article 329. https://doi.org/10.1186/1471-2180-10-329

Okada, N., Iida, T., Park, K. S., Goto, N., Yasunaga, T., Hiyoshi, H., Matsuda, S., Kodama, T., & Honda, T. (2009). Identification and characterization of a novel type III secretion system in trh-positive *Vibrio parahaemolyticus* strain TH3996 reveal genetic lineage and diversity of pathogenic machinery beyond the species level. *Infection and Immunity*, 77(2), 904-913. https://doi.org/10.1128/iai.01184-08

Osei-Adjei, G., Gao, H., Zhang, Y., Zhang, L., Yang, W., Yang, H., Yin, Z., Huang, X., Zhang, Y., & Zhou, D. (2017). Regulatory actions of ToxR and CalR on their own genes and type III secretion system 1 in *Vibrio parahaemolyticus*. *Oncotarget,* 8(39), 65809-65822. https://doi.org/10.18632/oncotarget.19498

Panwar, S., Kumari, S., Verma, J., Bakshi, S., Narendrakumar, L., Paul, D., & Das, B. (2023). Toxin-linked mobile genetic elements in major enteric bacterial pathogens. *Gut Microbiome*, 4, Article e5. https://doi.org/10.1017/gmb.2023.2

Paria, P., Kunal, S. P., Behera, B. K., Mohapatra, P. K. D., Das, A., Parida, P. K., & Das, B. K. (2019). Molecular characterization and genetic diversity study of *Vibrio parahaemolyticus* isolated from aquaculture farms in India. *Aquaculture*, 509, 104-111. https://doi.org/10.1016/j.aquaculture.2019.04.076

Park, K. S., Chong, Y., & Kim, M. K. (2016). Myricetin: biological activity related to human health. *Applied Biological Chemistry*, 59, 259-269. https://doi.org/10.1007/s13765-016-0150-2

Piplani, P., Sharma, M., Mehta, P., & Malik, R. (2018). N-(4-Hydroxyphenyl)-3, 4, 5-trimethoxybenzamide derivatives as potential memory enhancers: Synthesis, biological evaluation and molecular simulation studies. *Journal of Biomolecular*

Structure and Dynamics, 36 (7), 1867-1877. https://doi.org/10.1080/07391102.2017.1336943

Prithvisagar, K.S., Krishna Kumar, B., Kodama, T., Rai, P., Iida, T., Karunasagar, I., & Karunasagar, I. (2021). Whole genome analysis unveils genetic diversity and potential virulence determinants in *Vibrio parahaemolyticus* associated with disease outbreak among cultured *Litopenaeus vannamei* (Pacific white shrimp) in India. *Virulence*, 12(1), 1936-1949. https://doi.org/10.1080/21505594.2021.1947448

Raj, U., & Varadwaj, P. K. (2016). Flavonoids as multi-target inhibitors for proteins associated with Ebola virus: In silico discovery using virtual screening and molecular docking studies. Interdisciplinary Sciences: *Computational Life Sciences*, 8, 132-141. https://doi.org/10.1007/s12539-015-0109-8

Rajagopal, K., Byran, G., Jupudi, S., & Vadivelan, R. (2020). Activity of phytochemical constituents of black pepper, ginger, and garlic against coronavirus (COVID-19): an in silico approach. *International Journal of Health Allied Science*, 9(5), 43-50.

Rajagopal, K., Varakumar, P., Aparna, B., Byran, G., & Jupudi, S. (2021). Identification of some novel oxazine substituted 9-anilinoacridines as SARS-CoV-2 inhibitors for COVID-19 by molecular docking, free energy calculation, and molecular dynamics studies. *Journal of Biomolecular Structure and Dynamics*, 39(15), 5551-5562.

Rohl, C. A., Strauss, C. E., Misura, K. M., & Baker, D. (2004). Protein structure prediction using Rosetta. In *Methods in enzymology. Vol. 383* (pp. 66-93). Academic Press. https://doi.org/10.1016/S0076-6879(04)83004-0

Sajid Jamal, Q. M., Alharbi, A. H., & Ahmad, V. (2022). Identification of doxorubicin as a potential therapeutic against SARS-CoV-2 (COVID-19) protease: a molecular docking and dynamics simulation studies. *Journal of Biomolecular Structure and Dynamics*, 40(17), 7960-7974. https://doi.org/10.1080/07391102.2021.1905551

Semwal, D. K., Semwal, R. B., Combrinck, S., & Viljoen, A. (2016). Myricetin: A dietary molecule with diverse biological activities. *Nutrients*, 8(2), Article 90. https://doi.org/10.3390/nu8020090

Simpson, C. C. (2023). *Type VI secretion system facilitates intraspecies killing in Vibrio vulnificus via the associated rhs toxin/antitoxin system*. [MSc. Thesis, George Mason University] George Mason University. http://hdl.handle.net/1920/13316

Soto-Rodriguez, S. A., Lozano-Olvera, R., Montfort, G. R.-C., Zenteno, E., Sánchez-Salgado, J. L., Vibanco-Pérez, N., & Rendón, K. G. A. (2022). New insights into the mechanism of action of PirAB from *Vibrio Parahaemolyticus*. *Toxins*, 14(4), Article 243. https://doi.org/10.3390/toxins14040243

Trishala, A., Lakshmi, T., Rajeshkumar, S., Gurunathan, D., Geetha, R. V., & Roy, A. (2019). Physicochemical profile of *Acacia catechu* bark extract-*An invitro study. Indian Journal of Public Health Research & Development*, 10(11), 3513-3517.

Yadav, H., Mahalvar, A., Pradhan, M., Yadav, K., Sahu, K. K., & Yadav, R. (2023). Exploring the potential of phytochemicals and nanomaterial: A boon to antimicrobial treatment. *Medicine in Drug Discovery*, 17, Article 100151. https://doi.org/10.1016/j.medidd.2023.100151

Yang, Q., Dong, X., Xie, G., Fu, S., Zou, P., Sun, J., Wang, Y., & Huang, J., 2019. Comparative genomic analysis unravels the transmission pattern and intra-species divergence of acute hepatopancreatic necrosis disease (AHPND)-causing *Vibrio parahaemolyticus* strains. *Molecular Genetics and Genomics*, 294, 1007-1022. https://doi.org/10.1007/s00438-019-01559-7

Zhang, Q., Zhao, Y., Zhang, M., Zhang, Y., Ji, H., & Shen, L. (2021). Recent advances in research on vine tea, a potential and functional herbal tea with dihydromyricetin

and myricetin as major bioactive compounds. *Journal of Pharmaceutical Analysis*, 11(5), 555-563. https://doi.org/10.1016/j.jpha.2020.10.002

Zhang, Y., Gao, H., Osei-Adjei, G., Zhang, Y., Yang, W., Yang, H., Yin, Z., Huang, X., & Zhou, D. (2017). Transcriptional regulation of the type VI secretion system 1 genes by quorum sensing and ToxR in *Vibrio parahaemolyticus*. *Frontiers in Microbiology*, 8, Article 2005. https://doi.org/10.3389/fmicb.2017.02005